SECED 2023 Conference
Earthquake Engineering & Dynamics for a Sustainable Future
14-15 September 2023, Cambridge, UK

USING GROUND-MOTION SIMULATIONS WITHIN A MONTE CARLO APPROACH TO ASSESS PROBABILISTIC SEISMIC RISK

Archie RUDMAN[1], John DOUGLAS[2] & Enrico TUBALDI[3]

Abstract: *Accurate description of ground motion characteristics is a vital step in probabilistic seismic hazard and risk assessment. The growing number of ground motion models, and increased use of simulations in hazard and risk assessments, warrants a comparison between the different techniques available to predict ground motions. This research aims at investigating how the use of different ground-motion models can affect seismic hazard and risk estimates. For this purpose, a simple case study is considered, with a circular seismic source zone of a 100km radius, where earthquakes follow the Gutenberg-Richter relationship between magnitude 5 and 7.5. A stochastic ground-motion model is used within a Monte Carlo analysis to create a benchmark hazard output. This approach also allows the creation of a large number of records, removing the influence of potential deficiencies in the quality and quantity of empirical data when comparing models. Calculating the hazard with simulated ground motions helps to capture details of the ground-motion median and variability, which the fixed functional form of a ground motion prediction equation may fail to properly model. A variety of ground-motion models are then fitted to the simulated ground motion data. These include classic ground motion prediction equations (one with a basic functional form, another with a more complex form), and a model using an artificial neural network consisting of a single hidden layer of three nodes. The hazard is estimated from each of these models, with both fixed and magnitude-dependant standard deviations (sigmas) considered. This approach is extended to a risk assessment for an inelastic single-degree-of-freedom system. Results show the impact of ground-motion models on hazard and risk assessment estimates, with ground motions from larger events and from closer source-to-site distances having a larger influence on the results than expected.*

Introduction

Seismic risk expresses the expected probable losses due to shaking, measured through different metrics: e.g., economic, social, and environmental (e.g., Musson, 2000). The basis of estimating seismic risk is through a hazard analysis, which establishes the likelihood of earthquake ground motion of a given intensity occurring in the area under investigation. Probabilistic predictions of earthquake hazard and risk can be obtained via two distinct approaches: unconditional and conditional (e.g., Scozzese et al, 2020).

Unconditional methods use direct observations to estimate hazard and risk, an example of this being Monte Carlo hazard assessment (e.g., Musson, 2000). This method is noted for its adaptability, flexibility, and conceptual simplicity, and has been used frequently in research to good effect, such as EqHaz (Assatourians & Atkinson, 2013), a program to assess seismic hazard. Unconditional methods are considered more robust approaches to estimate risk; however, they are computationally expensive, meaning they are rarely used in practice. These techniques provide a good reference solution to evaluate different methods of carrying out a conditional risk assessment. Bradley et al. (2015) uses this direct method of estimating hazard and risk to compare the influence of different ground motion selection strategies when evaluating the peak displacement response of a nonlinear single degree of freedom system (SDOF). Scozzese et al. (2020) uses the outputs of Monte Carlo analyses as a reference solution to investigate the accuracy of a conditional method based on multiple stripe analysis.

Conditional methods, from now on referred to as ground-motion model (GMM)-based methods, are a more practice-orientated approach to estimate risk. Such methods include the Pacific Earthquake Engineering Research Centre's performance-based earthquake engineering approach (Moehle & Deierlein, 2004). Cornell (2005), among others, discusses both the benefits and drawbacks of this type of approach. These techniques require the definition of an intensity

[1] Mr, University of Strathclyde, Glasgow, United Kingdom, archie.rudman@strath.ac.uk
[2] Dr, University of Strathclyde, Glasgow, United Kingdom
[3] Dr, University of Strathclyde, Glasgow, United Kingdom

measure (IM) which describes the ground motion intensity at the site of interest. Seismic hazard can then be evaluated by characterising the seismic source zones of the site and combining this with a GMM, to fully describe the frequency of exceeding this IM during a time period of interest. The next step is to perform structural analyses for a given system to calculate its fragility of exceeding a given engineering demand parameter (EDP) at certain IM values. Finally, risk is estimated by convolving the results from both of these steps. It is worth noting here that this article uses two different terms to describe methods of predicting ground motion. Ground motion prediction equations (GMPEs) refer to traditional methods of predicting ground motions, i.e., those relying on regression analysis and a prescribed functional form, whereas GMM is used to refer to all models that predict ground motion.

One disadvantage of the unconditional approach is that it needs a large number of ground motions to be accurate; therefore, a method of simulating ground motions is required. Stochastic ground motion simulations model the randomness of the physical processes, and wave propagation, that cause ground motions thereby creating samples from just a few seismological inputs. This research uses the same terminology as Boore (2003), i.e. the general means of simulating ground motions is referred to as the stochastic *method*, whilst the specific application of this method is called a stochastic *model*. Stochastic methods can create a large number of records rapidly, helping to remove potential gaps and biases in empirical data. They have been used by Meirova et al. (2018) and Kowsari et al. (2021) to produce updated probabilistic seismic hazard assessments (PSHAs) for Israel and Iceland respectively.

Stochastic models can also be employed within GMM-based hazard assessments. Beauval et al. (2009) derives a hybrid deterministic–probabilistic GMM, based on simulated data using empirical Green's functions, for the island of Guadeloupe. The built model is compared with the Ambraseys et al. (2005) GMPE, but this is purely for illustrative purposes - as Douglas et al. (2006) showed that GMPE not to be well adapted for predicting earthquakes in the region. Stupazzini et al. (2020) integrated physics-based simulations into two different PSHAs and extended the hazard results to loss estimates of an artificial portfolio of buildings. Comparisons were made between the loss estimates produced from these two methods, which are also compared with estimates produced using the Chiou and Youngs (2014) GMPE.

When estimating hazard, and subsequently risk, GMM-based methods are far more prevalent in the literature - as seen by the ever-growing number, and variety, of GMMs (Douglas, 2022). However, it is difficult to make an effective comparison between the different GMM-based methods of risk assessment, especially with respect to the ability of the GMM to predict hazard. This is because there are a lack of high-quality ground motion data in many regions of the world (e.g., Xie et al., 2020) and so it is hard to establish an effective benchmark for models to be compared against.

This paper aims to compare the impact of using different GMMs on estimates of the seismic hazard, and subsequently risk. For this purpose, a stochastic model is employed within a fictive scenario to simulate ground motions, allowing the creation of benchmark hazard and risk estimates through the unconditional approach. The following sections describe the creation of this benchmark risk assessment as well as the construction of three GMMs, for use in GMM-based risk assessment. An empirical fragility curve is created from the stochastic model and a simple structural model, allowing risk to be estimated conditionally through a convolution with the hazard estimates from each of the GMMs. This procedure allows for direct comparison between each of the created GMMs, as well as proper judgements to be made on the impact that each GMM has on assessing risk, due to the benchmark created by the unconditional approach.

Seismic Scenario

For this study, a fictive scenario is established of a station at the centre of a 100km areal source zone, this background seismicity is used for simplicity, implying that the faults in the area are not known. Earthquakes in this zone follow the Gutenberg-Richter relationship between magnitude 5 and 7.5 – with a=4.5 and b=1.0. The Atkinson-Silva stochastic model (Atkinson & Silva, 2000) is implemented to obtain ground motions for this scenario, with spectral acceleration (*Sa)* values with 5% damping and a period of T=1s calculated. In total 100 sets of 100,000 simulations were created to form a hazard assessment, with this large number being used to demonstrate the uncertainties within the different GMMs.

Both magnitude and distance samples are generated based on their respective probability distributions to create ground-motion samples, when passed through the stochastic model. The distributions of the simulated magnitude, distance, and *Sa* are evaluated to ensure that they return expected and realistic values.

The assumption is made that the stochastic model used produces accurate and realistic ground motion intensities for this seismic scenario. This is justified by exercises that validate the stochastic method (e.g., Silva et al., 1996; Tsioulou et al., 2019). This allows the unconditional hazard and risk estimates from the stochastic model be considered the truth, and so act as a benchmark for the created GMMs to be compared against.

Ground-motion models

Separate to the unconditional analysis, the simulated ground motions are used to create three GMMs. This consists of basic and more complex GMPEs created through least squares regression analysis, with the functional form shown in equation (1) and equation (2) respectively:

$$\ln(Sa) = \mathrm{C}_0 + \mathrm{C}_1\mathrm{M} + \mathrm{C}_2 \ln(\mathrm{R}+5) \quad (1)$$

where $\mathrm{C}_0 = -9.3409, \mathrm{C}_1 = 1.6961$ and $\mathrm{C}_2 = -1.1043$

$$\ln(Sa) = \mathrm{C}_0 + \mathrm{C}_1\mathrm{M} + \mathrm{C}_2 \ln(\mathrm{R}+5) + \mathrm{C}_3\mathrm{M}^2 + \mathrm{C}_4\mathrm{R} \quad (2)$$

where $\mathrm{C}_0 = -18.2047, \mathrm{C}_1 = 5.0146, \mathrm{C}_2 = -1.3029, \mathrm{C}_3 = -0.2879$ and $\mathrm{C}_4 = 0.0038$

where M represents magnitude, R distance (km), and Sa is 5% damped spectral acceleration (g). A feedforward ANN is also considered, consisting of a single hidden layer of three nodes, with M and R as the input, and $ln(Sa)$ as output. The ANN uses the Levenberg–Marquardt optimisation technique (e.g., Dhanya & Raghukanth, 2018) and three nodes are used to prevent over-fitting (e.g., Derras et al, 2014).

Each of these GMMs are used in PSHA to predict ground motion intensity samples based on the simulated magnitude-distance combinations from the stochastic model. The GMM-based hazard analyses rely on the standard deviation (sigma) of each GMM to introduce variability in results when estimating *Sa*, whilst the unconditional approach already models the variability in ground motions by using every simulated record in the hazard analysis. For this study, only the total sigma is considered within the GMMs created.

Residual plotting of the three models indicated that magnitude-dependant sigmas could be considered (e.g., Youngs et al., 1997). As such, plotting magnitude (binned at 0.1 intervals) against sigma for each of these intervals showed a relationship between these two variables. An ANN (with a single hidden layer of two neurons) was fitted for each of the models to predict sigma based on magnitude. The ANN was selected to achieve the best fit of this data possible, ensuring accurate sigma prediction. A summary of the sigma values for each of these six considered models is presented in Table 1. The basic GMPE constructed has a higher sigma value than both the complex GMPE and ANN, implying it has a worse fit to the true ground-motion samples than the other two models. The sigmas are slightly smaller than generally observed for GMPEs obtained from actual ground-motion records. This is because the stochastic model does not include all sources of variability in earthquake ground motions.

Model	Sigma (natural logarithm)
Basic GMPE	0.5983
Basic GMPE (magnitude dependant sigma)	0.5936 – 0.5584
Complex GMPE	0.5932
Complex GMPE (magnitude dependant sigma)	0.5759 – 0.5455
ANN	0.5926
ANN with magnitude dependant sigma	0.5789 – 0.5340

Table 1. Comparing sigma values from the models created in this study.

Results

In this section, results from the GMM-based hazard models are presented and compared to each other, and to the results obtained using the Monte Carlo approach. This includes comparing the

returned median spectral acceleration values from the GMMs, a comparison of the hazard results produced by each of the models, and an investigation into the differences in these hazard results.

Predicting spectral acceleration

Median predictions from the three GMM-based models are plotted by the solid lines on Figure 1 for fixed distances of 25km and 75km, and fixed magnitudes of 5.75 and 6.75: with dashed lines on Figure 1 representing plus and minus one standard deviation from the median. Magnitude dependant sigma models are not included as median *Sa* predictions are not affected by this.

For the fixed distance plot, predictions from the ANN appear almost identical to that of the complex GMPE: whilst they vary significantly from the two GMPEs at smaller distances in the fixed magnitude plot. The similarities in model predictions occur at points where there is a wealth of magnitude and distance samples, with the differences appearing where fewer events are expected in the catalogue. The linear basic GMPE overpredicts *Sa* values for higher magnitudes and lower distances, with the differences between the complex GMPE and ANN more noticeable at shorter distances.

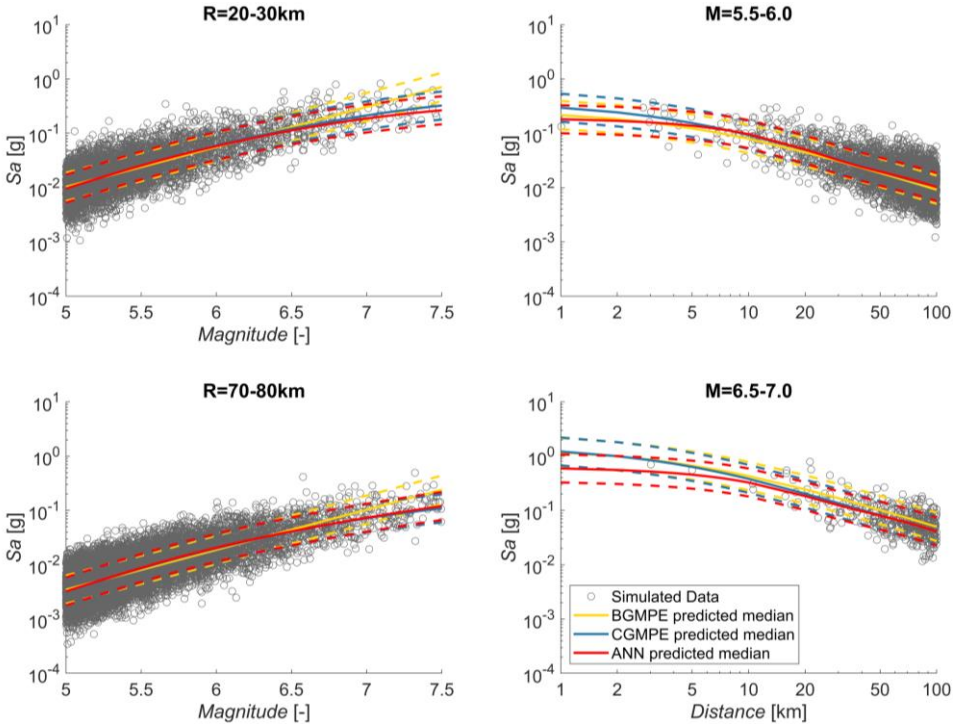

Figure 1. Median Sa predictions from all three GMM-based models (solid lines), at fixed distances of 25km and 75km, and fixed magnitude of 5.75 and 6.75, dashed lines represent plus and minus one standard deviation of the median.

Assessing hazard

Figure 2 shows the mean hazard curves for all created models: with dashed lines representing the 16th and 84th percentiles of the mean. The mean annual frequency of exceedance (MAF) is found by finding the number of ground motions that exceed a *Sa* threshold and multiplying it by the seismicity rate of the site: this is performed on a series of *Sa* thresholds for all 100 sets of records to obtain the MAF. The standard deviation of MAF of exceedance values is also computed, allowing the calculation of the 16th and 84th percentiles - assuming a lognormal distribution. All models appear to have a similar predictive quality at higher MAFs of exceedance but vary quite differently for lower MAFs. The magnitude dependant sigma models appear to not make any improvements on their fixed sigma alternatives, and so results from these models are discounted from further analysis.

Since these differences appear strong when using a wealth of simulated data, they will likely be even more significant when using real-world records, which are fewer in number and sparser in distribution. This indicates that GMM selection can be important when carrying out a hazard analysis, as these inaccuracies will be propagated through the risk assessment, leading to poorer loss estimations.

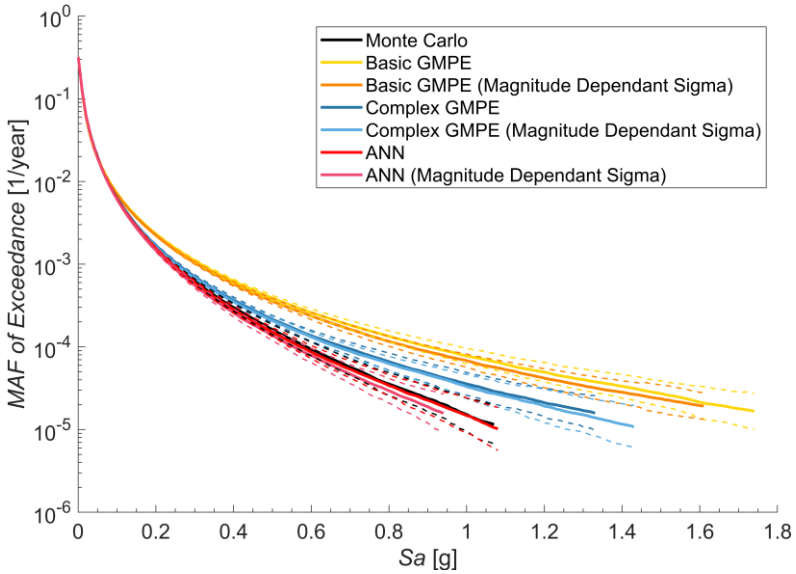

Figure 2. Mean hazard curves for all created models, solid lines show the mean hazard results whilst dashed lines show the 16th and 84th percentiles of the mean. Sa is plotted in a linear scale to better see differences between results.

To check whether the differences in hazard curves were persistent, the same procedure was carried out to predict *Sa* at a period of *T*=0.5s. Figure 3 presents the MAF of exceedance hazard curves for each of the models considered within this research, agreeing with the results from the hazard curves in Figure 2. As the differences between the GMM-based models and the benchmark hazard are similar, analysis of *Sa* at *T*=0.5s will not be further investigated.

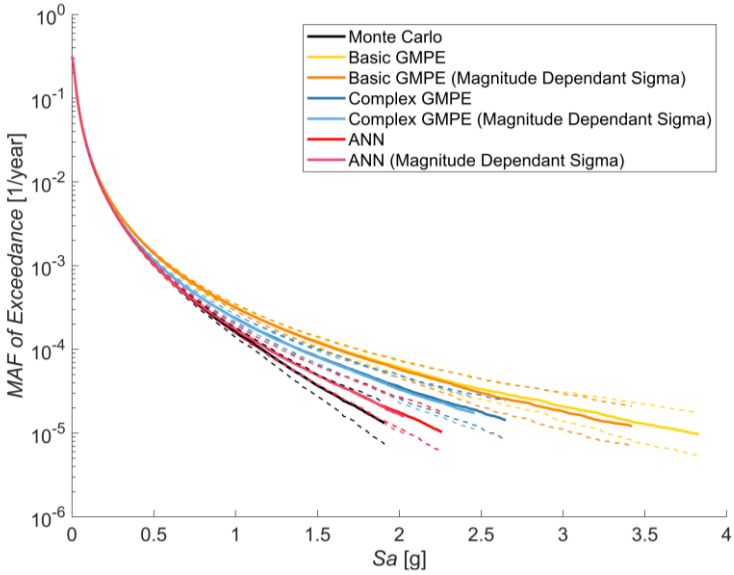

Figure 3. Mean hazard curves for all created models using Sa with a period of T=0.5s, solid lines show the mean hazard results whilst dashed lines show the 16th and 84th percentiles.

A different set of mean hazard results can also be obtained by finding the mean ground motion for a fixed set of MAF of exceedances. There is plenty of discussion on the suitability of these two approaches, which have been found to yield distinct hazard results (e.g., Bommer & Scherbaum, 2008). Interestingly, with the large suite of simulated data created by this study, both approaches to calculate the mean hazard yield very similar results, as shown in Figure 4. The only considerable difference in results between the two approaches is that the hazard curve created by finding the mean ground motion produces results with higher *Sa* and lower MAF of exceedance, with an increase of 25.66% in maximum *Sa* and decrease of 72.66% in minimum MAF of exceedance for the benchmark solution.

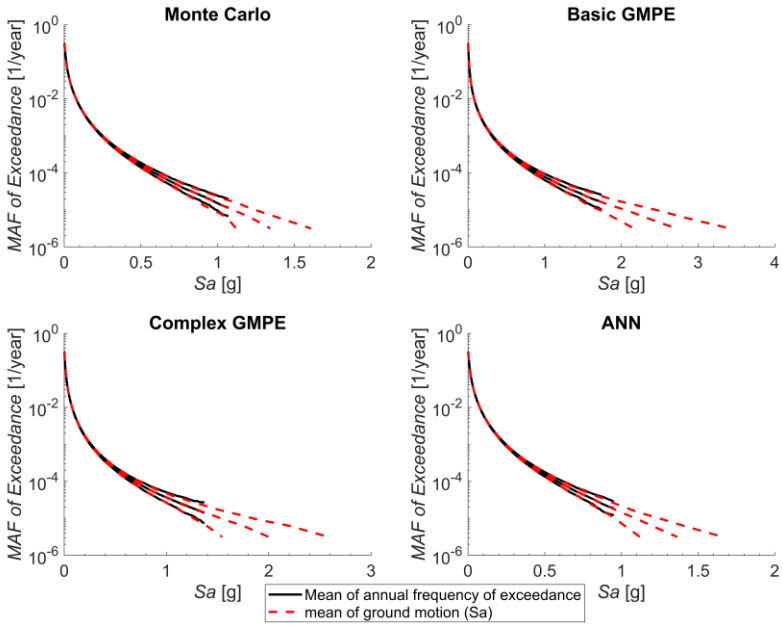

Figure 4. Comparison of mean hazard calculations via two approaches; calculating the mean of the annual frequency of exceedance; and calculating the mean Sa. Solid lines show the mean hazard, with dashed lines showing the 16th and 84th percentiles.

Evaluating differences between hazard results

The Kolmogorov–Smirnov (KS) test (e.g., Stephens, 1974) is used to compare results from the GMM-based hazard models against the benchmark hazard results. The test is carried out by finding the maximum absolute difference between two cumulative probability distributions (CDFs) tested. Although different techniques exist to compare hazard results such as Cohen's effective size (e.g., Malhotra, 2014), the KS test was chosen for its ease of application. As a non-parametric test, the KS test does not rely on the assumption and description of a probability distribution. It evaluates differences between the entire range of the two distributions, so it can ascertain differences at the extremes of the distribution, including stronger ground motions which are more likely to be different in the different hazard results.

The null hypothesis of the KS test is that the two CDFs are drawn from the same population. A CDF can be obtained from a hazard curve by first converting the frequency of exceedance for a range of *Sa* values to a probability. Given that the model assumes a Poisson process, equation (3) converts MAF of exceedance to annual probability of exceedance:

$$\mathrm{P} = 1 - \mathrm{e}^{-\lambda} \tag{3}$$

where P is the annual probability of exceeding a certain *Sa* value, and λ is the MAF of exceeding the same *Sa* value. One minus the annual probability of exceedance provides the CDF value for the given *Sa*. CDFs for each hazard model are obtained by performing this procedure on hazard results for *Sa* values at 0.01g intervals between 0g-6g. Each of the CDFs from the GMM-based approaches can then be tested against the CDF of the reference solution. Failing the test implies that the created GMM did not generate similar hazard estimates to the simulated data. This would imply that it would not be an appropriate model to use for risk assessment.

Table 2 presents the returned p-value of the KS test, with only the ANN model passing the test at the 5% confidence level – agreeing with the hazard curves. Thus, this is the only model that could be from the same distribution as the simulated data, and so provides the best prediction of hazard.

Model	Basic GMPE	Complex GMPE	ANN
P-value	<0.001	0.01	0.99
Reject null hypothesis?	✓	✓	×

Table 2. Results from Kolmogorov-Smirnov Test on the three GMM-based hazard models.

It is important to note that carrying out the KS test at different *Sa* interval spacing altered the result of the test. For instance, carrying out the test at intervals of 10^{-4}g spacing between 0g-6g rejected the null hypothesis for all three models; whilst using intervals of 0.1g for the same *Sa* bounds only rejected the null hypothesis for the basic GMPE. The interval spacing of 0.01g used to perform the test was considered acceptable for this scenario as this broader spacing is more likely to be used when comparing GMM-based hazard models to real world data. Nevertheless, further research should consider using other statistical tests to test the similarity between the hazard results, because of the sensitivity of the KS test.

Hazard Disaggregation

To investigate the differences in hazard predictions, hazard disaggregation (Bazzurro and Cornell, 1999) is performed. This breaks down the ground motions into their contributing factors (magnitude, distance, and epsilon) for the hazard. Figure 5 plots disaggregation results from both the Monte Carlo and GMM-based hazard analysis approaches for *Sa* values of 0.01g and 0.5g – mean magnitude and distance are also provided. Results are very similar at 0.01g, as expected by the agreement of the hazard curves (Figure 2) at this value of *Sa*. However, when disaggregation is performed at 0.5g, results vary between each of the models, as seen by differences in the plots.

The disaggregation results at 0.5g show a change in the dominant earthquake scenario. The mean magnitude-distance combination for the Monte Carlo-based approach at 0.01g is 5.71 and 56.59km, respectively, whilst at 0.5g this changes to 6.71 and 16.14km. At smaller magnitudes and further distances, the GMPEs accurately predict ground motions but at higher magnitudes and shorter distances, the GMPEs poorly predict the less abundant, stronger ground motions. This creates greater inaccuracies within the hazard assessment, which will lead to poor quality risk assessments, reaffirming the importance of GMM selection.

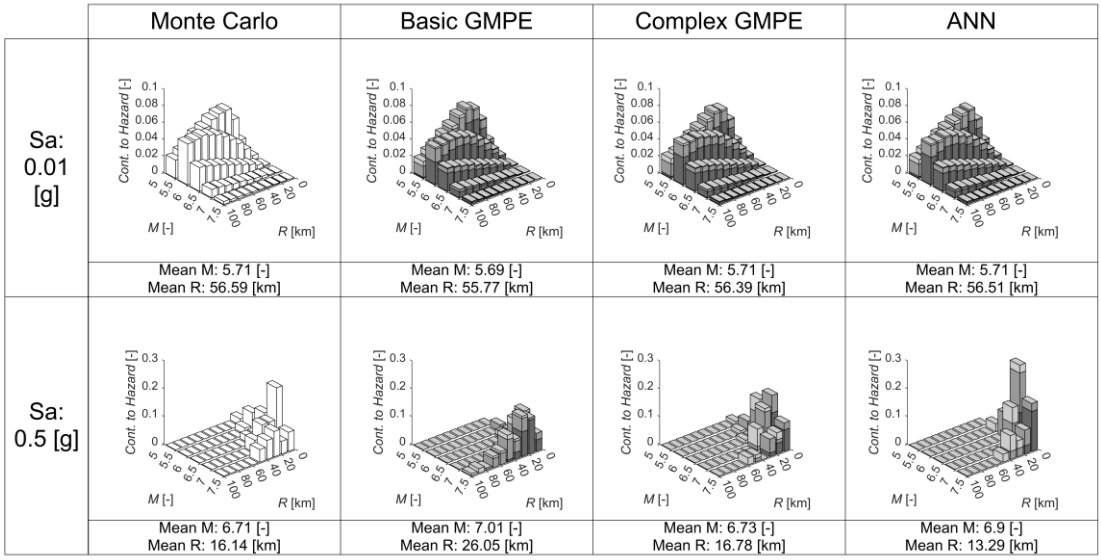

Figure 5. Hazard disaggregation results from the Monte Carlo-based approach and three GMM-based hazard assessment approaches, for Sa values of 0.01g and 0.5g.

Constricting magnitude and distance range of hazard results

Hazard disaggregation indicated that all models performed well at magnitudes 5.5-6.5 and distances of 10-50km, a parameter range which provides the ground motions of greatest interest from an engineering perspective. To confirm this agreement, hazard analysis is performed again on each of the models, but this time the scenario range is restricted to these magnitude and distance ranges, with the mean hazard results plotted on Figure 6.

When comparing the hazard curves created by this new, restricted, scenario, all models match quite well, with the ANN mirroring the true values for the whole range of values under investigation. This shows that the models are a good fit for the simulated data for this range of interest, and that discrepancies in hazard predictions between the models (when considering the whole range of magnitudes and distances), is likely down to the influence of ground motions caused by higher magnitudes and smaller distances, as suggested by hazard disaggregation.

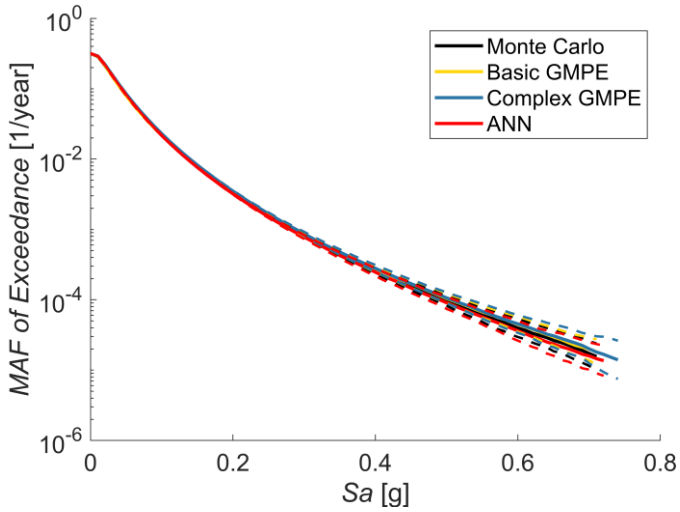

Figure 6. Mean hazard curves produced by the Monte Carlo-based hazard approach and three GMM-based hazard approaches, for a contracted distance of 10-50km and magnitude of 5.5-6.5, plotted by solid lines. Dashed lines show 16th and 84th percentiles of mean hazard.

Extension to risk assessment

To demonstrate the impact of ground-motion model selection on seismic risk assessment, each hazard model was extended to assess the risk on an inelastic SDOF system. This has elastic-perfectly plastic behaviour, with elastic period T=1s, and yield displacement u_y=0.03m. Nonlinear dynamic structural analyses were carried out for all 100 sets of ground-motion samples: calculating the maximum system displacement for each. Displacements are normalised by the system's yield threshold to produce the system ductility demand. The ductility threshold considered here is 4, this follows the assumption that the SDOF system is in the medium ductility class defined in Eurocode 8 (EN-1998-1).

For the unconditional Monte Carlo-based approach, seismic risk can be assessed by finding the annual frequency that this ductility threshold is exceeded; with the mean risk being the average rate that this threshold is exceeded for all 100 sets of records. Risk is estimated for the GMM-based hazard models by creating a fragility curve and combining this with the hazard results.

For the conditional approach, an empirical fragility curve is created by finding the conditional probability that the system ductility exceeds the threshold level, given the intensity measure of shaking. This is derived from the simulated hazard and ductility values and is shown in Figure 7. *Sa* is separated into 40 bins that are logarithmically spaced, with the bins presented by the dashed lines on Figure 7. The probability of exceeding the ductility threshold is calculated for each bin for all 100 sets of records – creating the mean cumulative distribution function shown.

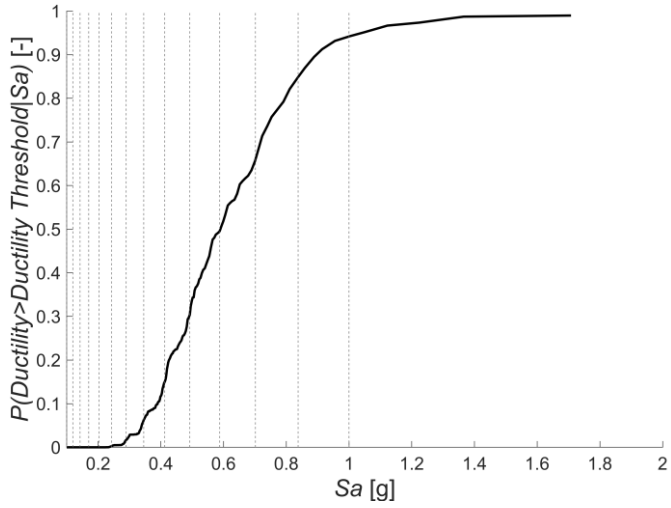

Figure 7. Created empirical fragility curve based on simulated values of Sa and ductility demand, dashed lines show the bins used to discretise Sa.

GMM-based risk estimates are made by convolving the fragility curve and the hazard curves for each GMM (e.g., Baker et al., 2021). Risk estimates for both the Monte Carlo based approach and GMM-based approaches are summarised in Table 3. The standard deviation and coefficient of variation (COV) for each model is also presented in Table 3: this value was obtained for each model by finding the risk from all 100 sets of simulations, allowing the calculation of the mean and standard deviation of risk and then the COV, which is the standard deviation divided by the mean.

Model	Monte Carlo	Basic GMPE	Complex GMPE	ANN
Mean risk	1.52×10^{-4}	3.49×10^{-4}	2.06×10^{-4}	1.47×10^{-4}
Standard deviation of risk	2.14×10^{-5}	2.21×10^{-5}	1.47×10^{-5}	1.44×10^{-5}
COV	0.14	0.06	0.07	0.10

Table 3. Summary of risk assessment results on the inelastic SDOF based on the four different hazard models, COV and standard deviation for each model is also provided.

The basic GMPE considerably overpredicts risk, with the estimate of 3.49×10^{-4} more than twice the benchmark value. Both the complex GMPE and ANN lead to better risk estimates, with the ANN better than the complex GMPE. The Monte Carlo based approach has a higher COV than the GMM-based approaches, with the basic GMPE providing the lowest COV. This is due to the reduced standard deviation for the complex GMPE and ANN, and the high mean value for the basic GMPE. This extension reinforces the results from the hazard assessment, demonstrating the importance of ground-motion model selection when carrying out a risk assessment.

Conclusions

A comparison of different methods of ground motion prediction has been carried out, in the context of their impact on hazard and risk estimates. A fictive scenario was established, with a stochastic model employed to simulate data to build these models. These simulations were used in a Monte Carlo analysis to directly estimate benchmark hazard and risk results. Three different methods of predicting ground motion were also considered: a basic and more complex classical GMPE, and an ANN. An empirical fragility curve was created from simulated ductility data, before being convolved with hazard results from each of the created GMMs to evaluate their impact on risk.

It was shown that careful selection of a GMM is required to obtain the best estimates of seismic risk. Out of the three GMMs created, only the ANN appears to produce hazard estimates similar to the benchmark results, and the same outcome is visible from the risk estimates. Although it is important to note that ANNs are only successful when trained on large, complete, datasets - something that is hard to replicate in the real world.

Hazard disaggregation was performed on each hazard model. With the GMMs struggling to predict high magnitude, short distance, events at higher IM levels, causing the over-prediction of hazard, and ultimately risk. It may be possible to partially reduce this problem by using more complex functional forms, but these are difficult to constrain without large datasets. Inefficient risk estimates may result in inaccurate design, and ill-informed decision making. If estimates are poor in a data-rich scenario, they will be worse in the real world where data are less comprehensive.

References

BS EN 1998-1:2004+A1:2013, *Eurocode 8: Design of structures for earthquake resistance – Part 1: General rules, seismic actions and rules for buildings*, AMD 31st May 2013

Ambraseys, NN, Douglas, J, Sarma, SK & Smit, PM 2005. Equations for the estimation of strong ground motions from shallow crustal earthquakes using data from Europe and the Middle East: Horizontal peak ground acceleration and spectral acceleration. *Bulletin of Earthquake Engineering,* 3**,** 1-53.

Assatourians, K & Atkinson, GM 2013. EqHaz; An Open-Source Probabilistic Seismic-Hazard Code Based on the Monte Carlo Simulation Approach. *Seismological Research Letters,* 84**,** 516-524.

Atkinson, GM & Silva, W 2000. Stochastic modeling of California ground motions. Bulletin of the Seismological Society of America, 90, 255-274.

Baker, J., Bradley, B., & Stafford, P. (2021). Seismic Hazard and Risk Analysis. Cambridge: Cambridge University Press. doi:10.1017/9781108425056

Bazzurro, P & Cornell, CA 1999. Disaggregation of seismic hazard. Bulletin of the Seismological Society of America, 89, 501-520.

Beauval, C, Honoré, L & Courboulex, F 2009. Ground-Motion Variability and Implementation of a Probabilistic–Deterministic Hazard MethodGround-Motion Variability and Implementation of a Probabilistic–Deterministic Hazard Method. *Bulletin of the Seismological Society of America,* 99**,** 2992-3002.

Bommer, JJ & Scherbaum, F 2008. The Use and Misuse of Logic Trees in Probabilistic Seismic Hazard Analysis. *Earthquake Spectra,* 24**,** 997-1009.

Bradley, BA, Burks, LS & Baker, JW 2015. Ground motion selection for simulation-based seismic hazard and structural reliability assessment. *Earthquake Engineering & Structural Dynamics,* 44**,** 2321-2340.

Chiou, BSJ & Youngs, RR 2014. Update of the Chiou and Youngs NGA Model for the Average Horizontal Component of Peak Ground Motion and Response Spectra. Earthquake Spectra, 30, 1117-1153.

Cornell, C 2005. On earthquake record selection for nonlinear dynamic analysis. Luis Esteva Symposium

Derras, B, Bard, PY & Cotton, F 2014. Towards fully data driven ground-motion prediction models for Europe. Bulletin of Earthquake Engineering, 12, 495-516.

Dhanya, J & Raghukanth, STG 2018. Ground Motion Prediction Model Using Artificial Neural Network. Pure and Applied Geophysics, 175, 1035-1064.

Douglas, J, Bertil, D, Roulle, A, Dominique, P & Jousset, P 2006. A preliminary investigation of strong-motion data from the French Antilles. Journal of Seismology, 10, 271-299.

Douglas, J & Edwards, B 2016. Recent and future developments in earthquake ground motion estimation. Earth-Science Reviews, 160, 203-219.

Kowsari, M, Halldorsson, B, Snaebjornsson, JT & Jonsson, S 2021. Effects of different empirical ground motion models on seismic hazard maps for North Iceland. Soil Dynamics and Earthquake Engineering, 148, 106513.

Malhotra, PK 2014. Cost of Uncertainty in Seismic Hazard.

Meirova, T, Shapira, A & Eppelbaum, L 2018. PSHA in Israel by using the synthetic ground motions from simulated seismicity: the modified SvE procedure. Journal of Seismology, 22, 1095-1111.

Moehle, J & Deierlein, GG 2004. A framework methodology for performance-based earthquake engineering.

Musson, RMW 2000. The use of Monte Carlo simulations for seismic hazard assessment in the UK. Annals of Geophysics, 43**,** 1-9.

Scozzese, F, Tubaldi, E & Dall'asta, A 2020. Assessment of the effectiveness of Multiple-Stripe Analysis by using a stochastic earthquake input model. Bulletin of Earthquake Engineering, 18**,** 3167-3203.

Silva, WJ, Abrahamson, N, Toro, G & Constantino, C 1996. Description and validation of the stochastic ground motion model.

Stephens, MA 1974. Edf Statistics for Goodness of Fit and Some Comparisons. *Journal of the American Statistical Association,* 69**,** 730-737.

Stupazzini, M, Infantino, M, Allmann, A & Paolucci, R 2021. Physics-based probabilistic seismic hazard and loss assessment in large urban areas: A simplified application to Istanbul. *Earthquake Engineering & Structural Dynamics,* 50**,** 99-115.

Tsioulou, A, Taflanidis, AA & Galasso, C 2019. Validation of stochastic ground motion model modification by comparison to seismic demand of recorded ground motions. *Bulletin of Earthquake Engineering,* 17**,** 2871-2898.

Xie, YZ, Sichani, ME, Padgett, JE & Desroches, R 2020. The promise of implementing machine learning in earthquake engineering: A state-of-the-art review. *Earthquake Spectra,* 36**,** 1769-1801.

Youngs, RR, Chiou, SJ, Silva, WJ & Humphrey, JR 1997. Strong Ground Motion Attenuation Relationships for Subduction Zone Earthquakes. *Seismological Research Letters,* 68**,** 58-73.